Tribology Letters (2022) 70: 88
https://doi.org/10.1007/s11249-022-01630-2

ORIGINAL PAPER

On the Electric Contact Resistance

B. N. J. Persson[1,2]

Received: 4 May 2022 / Accepted: 28 June 2022 / Published online: 20 July 2022
© The Author(s) 2022

Abstract
When an electric current flow across an interface between two contacting solids a change in the electric potential occur over the interface. One part of the electric contact resistance is due to the constrictions at asperity contact regions. Barber has shown that the constriction resistance can be related to the interfacial contact stiffness. I discuss the relation between the classical (approximate) Holm theory for the constriction resistance and the (exact) theory involving the contact stiffness.

Graphical Abstract

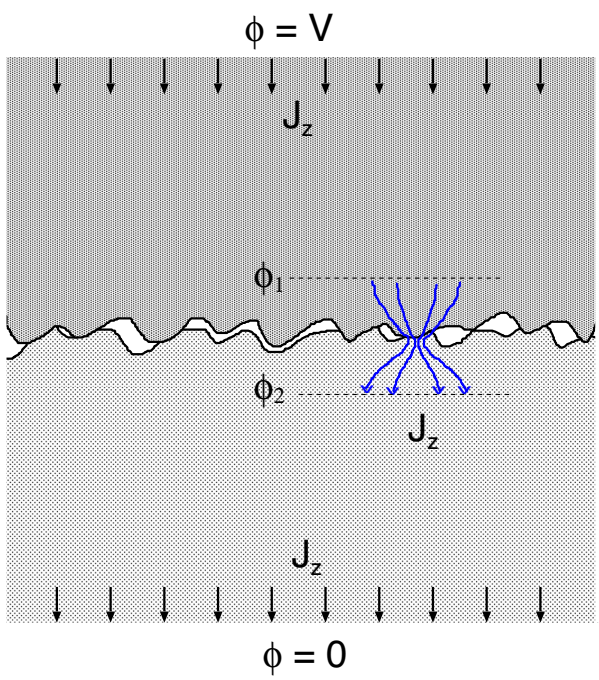

Keywords Contact resistance · Contact stiffness · Surface roughness · Constriction · Metallic · Interfacial separation

1 Introduction

The electric contact between metallic bodies is often a weak link in electronic devices [1]. Thus surface roughness and thin oxide or contamination films may have a huge influence on the nature of an electric contact. In general, if a current I flow through the interface between two solids a finite voltage drop U occur over the interface. The contact

✉ B. N. J. Persson
b.persson@fz-juelich.de

1 Peter Grünberg Institute (PGI-1), Forschungszentrum Jülich, 52425 Jülich, Germany

2 Multiscale Consulting, Wolfshovener str. 2, 52428 Jülich, Germany

resistance $R = U/I$. Holm has developed a theory to predict the constriction resistance assuming an idealized distribution of contact regions [2–4]. However, the distribution of contact regions is in general not known and it is not always clear how to apply the theory of Holm to practical situations.

Barber has shown that a detailed knowledge of the contact morphology is not necessary for predicting the contact resistance [5, 6]. Using a very general argument he showed that the constriction resistance can be related to the mechanical contact stiffness. The latter can be calculated accurately using e.g. the Persson contact mechanics theory [7–11]. This theory shows that the contact stiffness often is determined by the most long-wavelength roughness, which may deform elastically rather than plastically. In this work I will discuss the relation between the Holm and Barber approaches to the contact resistance problem.

2 Surface Roughness Power Spectra

The statistical properties of randomly rough surfaces are fully determined by the surface roughness power spectrum $C(\mathbf{q})$ (see Refs. [12–14]). The power spectrum is proportional to the square of the absolute value of the two-dimensional Fourier transform of the surface height function $z = h(x, y)$. Thus, the power spectra is a function of the wavevector $\mathbf{q} = (q_x, q_y)$. For surfaces with isotropic roughness $C(\mathbf{q})$ depends only on the magnitude $q = |\mathbf{q}| = 2\pi/\lambda$ of the wavevector. Here λ is the wavelength of a roughness component. From $C(\mathbf{q})$ standard quantities such as the root-mean-square (rms) roughness amplitude h_{rms} or the rms-slope ξ of the surface can be easily calculated.

Most engineering objects have some particular shape, with otherwise smooth surfaces on the length scale of the objects. Such surfaces have a power spectra with a small wavenumber (or long wavelength) roll-off region, and on a log-log scale $C(q)$ typically looks like the blue line in Fig. 1. This is in contrast to many natural surfaces, e.g., the surface of a fractured granite stone, which have roughness on all length scale up to the linear size of the object. Such surfaces have power spectra without a roll-off region (see red line in Fig. 1). Here we will consider surfaces with roll-off regions unless otherwise stated.

Note that both power spectra in Fig. 1 depend nearly linearly on the wavenumber for large wavenumber on the log–log scale. This is typical for self-affine fractal surface and the slope $= -2 - 2H$ of the lines define the Hurst exponent H (or fractal dimension $D_{\mathrm{f}} = 3 - H$).

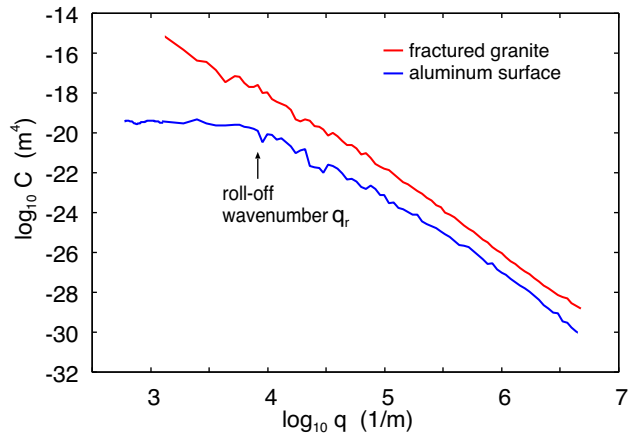

Fig. 1 The surface roughness power spectrum of a granite surface produced by fracture (red) and for the surface of a die casted aluminum structure (blue). The roll-off wavenumber q_{r} is indicated (Color figure online)

3 Contact Area and the Average Interfacial Separation

Consider the contact between two elastic solids with nominally flat surfaces. Because of surface roughness the contact will not be complete. As long as the relative contact area A/A_0 (where A_0 is the nominal contact area) is below ≈ 0.3 the contact area increases approximately linearly with the applied squeezing pressure p. Theory and numerical simulations shows that [7, 15–17]

$$\frac{A}{A_0} \approx \frac{2p}{\xi E^*}, \tag{1}$$

where ξ is the rms slope of the combined roughness profile and where the effective elastic modulus E^* is determined by the Young's elastic modulus and the Poisson ratio of the two solids via $1/E^* = (1 - \nu_1^2)/E_1 + (1 - \nu_2^2)/E_2$.

In many applications the (relative) area of real contact is very small and the surfaces are separated by an air film in most places. The resulting gap field (surface separation) between two solids is very important for many applications, but for the contact resistance the average gap height (average surface separation) $\bar{u}$ is enough. When the applied pressure p is such that the relative contact area is much less than 1 (but not so small that finite size effects become important), the average separation $\bar{u}$ is related to the squeezing pressure p as [8]

$$p \approx \beta E^* e^{-\bar{u}/u_0} \tag{2}$$

where $u_0 \approx h_{\mathrm{rms}}/2$ and β both are determined by the surface roughness power spectrum $C(\mathbf{q})$. The theory also predicts

the probability distribution of stress and surface separation [10, 11].

4 Interfacial Contact Stiffness

Because of surface roughness an interface of solid contact is usually less stiff than the bulk material, and is often represented as a layer of (nonlinear) elastic springs. If two solids with a nominally flat surfaces are squeezed together with the pressure p the normal interfacial contact stiffness is defined as $K = -dp/d\bar{u}$. If the pressure is not too high (as to approach complete contact) or too low (where finite-size effects become important) then for elastic contact (2) holds and

$$K \approx \frac{1}{u_0}\beta E^* e^{-\bar{u}/u_0} = \frac{p}{u_0} \tag{3}$$

In Fig. 2 we show the calculated result for the contact stiffness over a wide pressure range where both finite-size effects and approach of complete contact occur [18, 20]. For pressures above the finite-size regime the stiffness is well approximated by $K = (p/u_0)\exp(cp/E^*)$. In the finite size region $K \sim p^{1/(1+H)}$ (see Refs. [18, 19]). The onset of this low-pressure scaling regime moves to lower pressure when the roll-off region in the power spectrum increases. In the finite-size regime the solids makes contact only at the highest macro asperity [18].

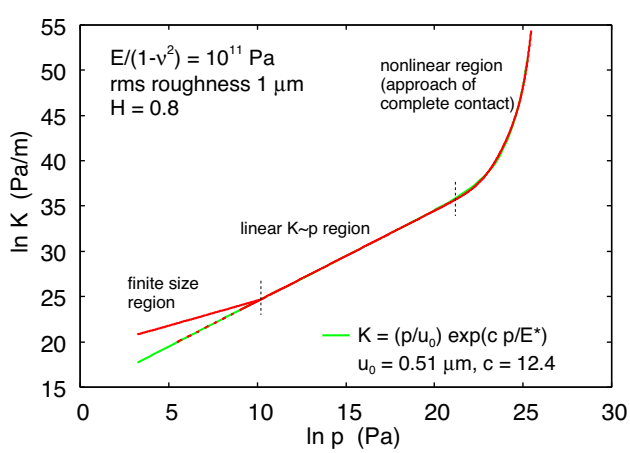

Fig. 2 Red line: The calculated perpendicular interfacial contact stiffness K as a function of the squeezing pressure p (ln-ln scale). For an elastic solid with $E^* = E/(1-\nu^2) = 100$ GPa and with a randomly rough (self affine fractal) surface with the rms-roughness amplitude 1 µm and Hurst exponent $H = 0.8$. For pressures above the finite-size regime the stiffness is well approximated by $K \approx (p/u_0)\exp(cp/E^*)$ (green line) and in the finite-size regime $K \sim p^{1/(1+H)}$ (see Refs. [18, 19]). The parameter $u_0 \approx h_{\mathrm{rms}}/2$ and c is given approximately as $c \approx (4.4 - 33H + 50H^2)/(h_{\mathrm{rms}}q_{\mathrm{r}})$ for $0.5 < H < 1$ (Color figure online)

The contact stiffness theory has been tested experimentally for both for elastically soft materials like rubber [21, 22], and for elastically stiff materials [23, 24]. In both cases a linear dependency of the stiffness on the squeezing pressure was found with $K \approx p/u_0$ with $u_0 \approx h_{\mathrm{rms}}/2$. For metals plastic flow is expected at the asperity level, which will effectively increases the stiffness. For elastically stiff solids and for small applied squeezing forces, finite size effects are important and the contact resistance will depend nonlinearly on the applied force as observed in some cases.

Note that h_{rms} and hence the contact stiffness are determined mainly by the longest wavelength roughness, and in most cases it is not necessary to study the surface topography $h(x, y)$ at high magnification in order to obtain the contact stiffness.

5 Relation Between Contact Stiffness and Contact Resistance

If an electric potential is applied between two metallic solids in contact an electric current will flow from one solid to the other via the asperity contact regions (see Fig. 3). The interfacial resistance to the current flow is denoted as the electric contact resistance. The electric contact conductance α_{el} is defined by

$$J_z = \alpha_{\mathrm{el}}(\phi_1 - \phi_2), \tag{4}$$

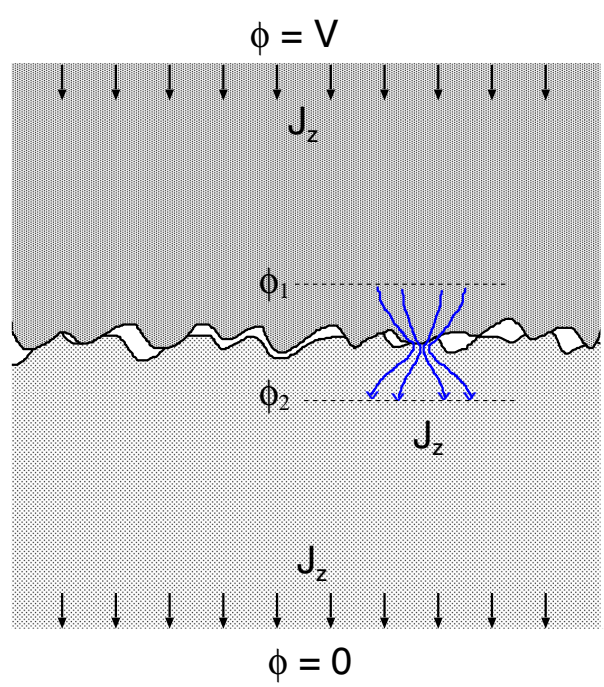

Fig. 3 The electric current at the interface is highly non-uniform but becomes nearly uniform a short distance from the interface where the electric potential is ϕ_1 in solid 1 and ϕ_2 in solid 2

where J_z is the electric current and ϕ_1 and ϕ_2 are the electric potential in the two solids close to the interface, at such distance from the interface that the electric potential is nearly uniform in the plane parallel to the interface. In a similar way one can define a thermal contact conductance by $J_z = \alpha_{\rm th}(T_1 - T_2)$, where J_z is the thermal current, and $T_1 - T_2$ the temperature change over the interface. The contact resistance $R = 1/(\alpha A_0)$ (here we assume $\alpha = \alpha_{\rm el}$ or $\alpha_{\rm th}$ are constant in the nominal contact area A_0).

It has been shown by Barber [5] (see also Refs. [20, 25]) that the constriction contribution to the heat and electric contact resistance are closely related to the mechanical contact stiffness K. The fundamental reason for this is the similarities between the equations determining elastic deformations and the temperature in thermal contact, and the electric potential in electric contacts. For the latter two phenomena conservation of heat and of electric charge gives $\nabla \cdot \mathbf{J} = 0$ where $\mathbf{J} = -\kappa_{\rm th}\nabla T$ for the heat current and $\mathbf{J} = -\kappa_{\rm el}\nabla\phi$ for the electric current. This gives $\nabla^2 T = 0$ and $\nabla^2\phi = 0$, respectively. These equations are similar to the continuum mechanics equation determining elastic deformations in the static limit. In particular, Boussinesq has shown that if an elastic halfspace is loaded by a normal stress, the solution involves a function ψ which satisfies $\nabla^2\psi = 0$. Using this one can show that [5]

$$\alpha_{\rm el} = 2\kappa^*_{\rm el}\frac{K}{E^*} \tag{5}$$

$$\alpha_{\rm th} = 2\kappa^*_{\rm th}\frac{K}{E^*}, \tag{6}$$

where $1/\kappa^*_{\rm el} = 1/\kappa^{(0)}_{\rm el} + 1/\kappa^{(1)}_{\rm el}$ where $\kappa^{(0)}_{\rm el}$ and $\kappa^{(1)}_{\rm el}$ are the electric conductivity of solid 1 and 2, respectively. The effective thermal conductivity $\kappa^*_{\rm th}$ is defined in a similar way.

Since the mechanical contact stiffness is mainly determined by the long wavelength roughness, it follows that the same is true for the constriction contribution to the electric and the thermal contact resistance. Thus information about the short wavelength roughness is in most cases not needed when determining the electrical and thermal contact resistance. Since the area of real contact is determined mainly by the short wavelength roughness, and since the (elastic) contact area would vanish if roughness down to arbitrary short length scale would exist, one could theoretically imagine a case where the electric contact resistance is finite even when the area of real contact would vanish. In this case an infinite electric current density would flow through a zero contact area in such a way that $\infty \times 0 = I$ where the electric current $I = U/R$. In reality this is of course is impossible since there is a short distance cut-off which must be larger than an atomic dimension. Furthermore, as the contact area decreases the contact pressure increases (given a fixed normal load) and finally plastic deformation of the solids will occur and the contact area saturates.

In many cases plastic deformation does not occur at the (long) length scales which determines the contact stiffness and the constriction resistance. In these cases the constriction resistance is accurately obtained assuming only elastic deformations, even if plastic deformations occur at short length scales.

The results presented above assume that the contact resistance is entirely due to the current constrictions involving homogeneous materials and no contamination or oxide films. Thin oxide and contamination films could affect the electric contact resistance hugely, unless the local contact pressure is big enough to break-up these films [3]. If there are no strong bonds formed at the interface between the solids, contamination and oxide films could also strongly increase the contact heat resistance because of weak interfacial coupling, even if the thermal conductivity of such films are high. In addition, the non-contact area could be very important for heat transfer via heat diffusion in the surrounding gas, or via blackbody heat radiation, which can be strongly enhanced at short surface separation because of the near field (evanescent) part of the electromagnetic field [25–27].

6 Electric Contact Resistance

If we assume that the pressure $p = p_0$ is constant in the nominal contact area, and if we assume $K = p_0/u_0$ and denote the potential drop over the interface by $U = \phi_1 - \phi_2$ from (4) and (5) we get

$$J_z = 2\kappa^*_{\rm el}\frac{p_0}{u_0 E^*}U \tag{7}$$

The electric current

$$I = J_z A_0 = 2\kappa^*_{\rm el}\frac{p_0 A_0}{u_0 E^*}U \tag{8}$$

Since $p_0 A_0 = F$ is the normal force, we obtain the constriction resistance

$$R = \frac{U}{I} = \frac{E^*}{2F}\rho^* u_0 \tag{9}$$

where the resistivity $\rho^* = 1/\kappa^*_{\rm el}$. If the material on both sides of the junction are identical materials then $\kappa^*_{\rm el} = \kappa_{\rm el}/2$ and $\rho^* = 2/\kappa_{\rm el} = 2\rho$ and $E^* = E/[2(1-\nu^2)]$.

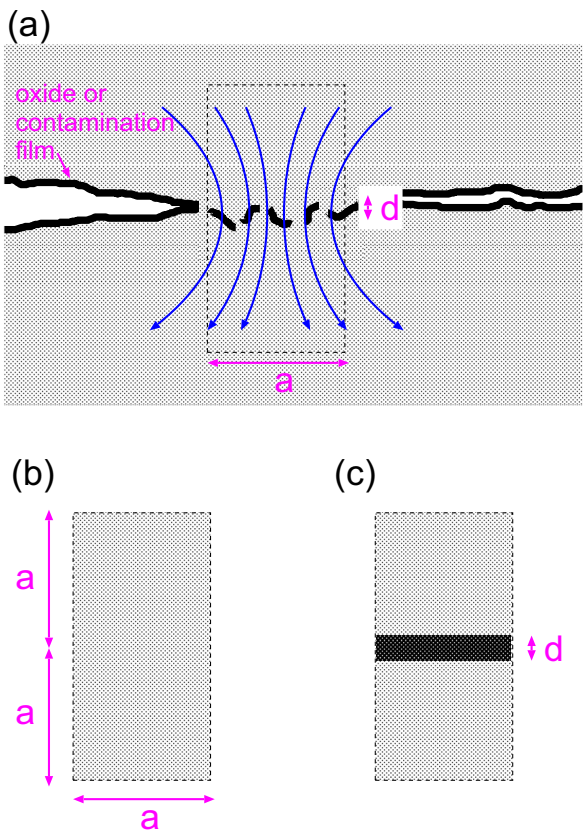

Fig. 4 **a** The electric current at one asperity contact region. **b** Most of the energy dissipation occur in a volume element of linear size a at the junction, giving the resistence $\sim \rho a/a^2 = \rho/a$ where ρ is the resistivity of the bulk material. **c** If a thin layer (thickness d) of material with different resistivity ρ_f occur at the interface there will be an additional contribution to the resistance given by $\rho_f d/A \sim \rho_f d/a^2$

7 Classical Theory for the Contact Resistance

The classical theory of the constriction resistance is presented in the book of Holm [3]. The most basic result is the resistance of a circular constriction which can be derived in different ways which we first briefly review.

Consider a circular contact region between two conducting semi-infinite solids. Figure 4a shows the electric current flow through the contact region. We assume first that there is no isolating (oxide or contamination) film at the interface between the two solids. For this case the resistance is entirely due to the constriction and there are several ways to estimate this resistance:

(1) There are only two quantities in the problem, namely the electric resistivity ρ and the diameter of the circular constriction a, and the only way to construct a variable with the dimension of the resistance is ρ/a so we expect from dimensional arguments

$$R = \alpha \frac{\rho}{a} \tag{10}$$

where α is a number of order unity.

(2) Most of the energy dissipation occur in a volume element of linear size a at the junction, where $A \sim a^2$ is the cross section area of the junction (see Fig. 4b). The electric resistance of a cylinder of width a and height $\sim a$ is $\sim \rho a/A \sim \rho/a$ where ρ is the resistivity of the bulk material. Thus we expect again a contact resistance of the form (10).

(3) If one assumes that the electric current flow radially (and angular uniform) away from the constriction then the contact resistance of a thin shell between r and $r + dr$ is $\rho dr/(2\pi r^2)$ and the total contact resistance

$$R \approx 2 \int_a^\infty \frac{\rho dr}{2\pi r^2} = \frac{1}{\pi}\frac{\rho}{a} \tag{11}$$

which is again on the form (10).

(4) The exact solution [28] is obtained by solving the Laplace equation for the electric potential, $\nabla^2 \phi = 0$ with appropriate boundary conditions. If a is the diameter of the circular contact region then this approach gives (10) with $\alpha = 1$.

We note that the result (10) (with $\alpha = 1$) is valid for a circular contact between two semi-infinite solids with flat surfaces. Hence it does not take into account the geometrical shape of the asperities from which the contact region is derived. In the Barber approach this shape-factor is in principle included (in the small slope approximation).

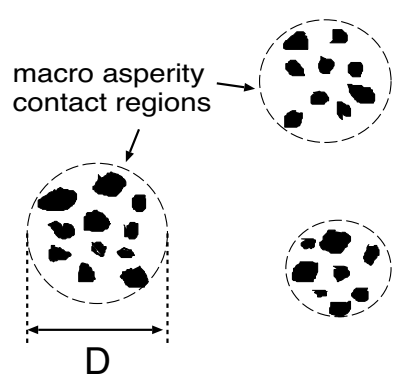

Fig. 5 The contact morphology when two nominally flat elastic solids are squeezed into contact consist in general (unless the contact pressure is very high) of well separated macroasperity contact regions. Each such region consist of closely spaced contact spots (with the average diameter $\bar{a}$) which are denoted microasperity contact regions. From the point of view of the contact constriction contribution to the resistance, the macroasperity contact regions can be considered as compact islands with a radius D indicated by the dashed circles

Figure 5 shows the contact morphology when two nominally flat elastic solids, with surface roughness power spectra with roll-off regions, are squeezed into contact. In general, the contact consist (unless the contact pressure is very high) of many well separated islands (macroasperity contact regions), each consisting of many closely spaced contact spots.

Consider now a macroasperity contact region (diameter D) and assume that N microasperity contact regions (with the average diameter $\bar{a}$) are uniformly distributed within it (see Fig. 5). In that case the contact resistance of the macroasperity contact region is approximately [2–4]

$$R \approx \frac{\rho}{N\bar{a}} + \frac{\rho}{D} \tag{12}$$

Since in general the microasperity contact regions are densely distributed within the macroasperity contact region it is easy to see that the contact resistance is determined mainly by the term ρ/D. This result is consistent with the fact that the constriction resistance is determined by the long wavelength roughness and hence the internal structure of the macroasperity contact regions (which is determined by shorter wavelength roughness) is unimportant.

Consider now a system with N' macroasperity contact regions. If the applied load is not too high then the distance between the macroasperity contact regions will be large and the interaction between them can be neglected. In that case the total resistance will be a factor of $1/N'$ smaller than given by (12):

$$R \approx \frac{\rho}{N'D} \tag{13}$$

Since in a large pressure range, where the contact area is proportional to the contact pressure, N' is proportional to the applied normal force F and hence R is proportional to $1/F$ as also found in the more accurate approached based on the Barber theory for the contact resistance.

8 Comparing the Expressions for the Constriction Resistance

Let us compare (9) with (13):

$$R \approx \frac{E^*}{2F}\rho^* u_0, \qquad R \approx \frac{\rho^*}{2N'D}.$$

The size and the concentration of the macroasperity contact regions can be estimated using the Greenwood-Williamson (GW) theory [29] if we assume that the pressure is so small that the contact regions are separated enough that the elastic interaction between the contact regions can be neglected. In fact, the contact stiffness is only (approximately) correctly described by the GW theory if the contact regions are separated by distances in the order of or larger than the roll-off wavelength in the power spectrum [30].

Assuming the height probability distribution $P(z) \sim \exp(-\gamma z/h_{\mathrm{rms}})$, where γ is a number of order unity (typically $\gamma \approx 2$, see [31]), the GW theory predict that

$$F = \frac{2(2\pi)^{1/2}}{3\gamma} E^* N' D h_{\mathrm{rms}} \tag{14}$$

If we choose $\gamma = (2/3)(2\pi)^{1/2} \approx 1.7$ we get from (13) and (14) the result (9) obtained using the rigorous Barber approach. We do note, however, if one assumes a Gaussian distribution of asperity heights, as expected for a randomly rough surface, then the GW theory does not predict a strict linear relation between F and N'.

9 Discussion

Assume that there is a thin film, e.g., an oxide film or a contamination film, at the interface between the two solids. We can estimate the contribution from this film to the contact resistance using the picture shown in Fig. 4c. Thus, if a thin layer (thickness d) of material with different resistivity ρ_{f} occur at the interface there will be an additional contribution to the resistance given by

$$R_{\mathrm{f}} = \frac{\rho_{\mathrm{f}} d}{A} \tag{15}$$

and the total resistance is the sum of (15) and the constriction resistance (9):

$$R_{\mathrm{tot}} \approx \frac{E^*}{2F}\rho^* u_0 + \frac{\rho_{\mathrm{f}} d}{A}$$

We can use this expression to estimate when the interfacial film will dominate the resistance. The interfacial film will give the same contribution as the constrictions when

$$\frac{E^*}{2F}\rho^* u_0 = \frac{\rho_{\mathrm{f}} d}{A}$$

In most cases of interest plastic deformation determine the area of real contact so that $\sigma_{\mathrm{P}} A = F$ and we get

$$\rho_{\mathrm{f}} = \frac{E^*}{\sigma_{\mathrm{P}}} \frac{u_0}{d} \rho$$

In a typical case $u_0 \approx 1$ µm, $d \approx 1$ nm, $E^* \approx 100$ GPa and $\sigma_{\mathrm{P}} \approx 1$ GPa giving

$$\rho_{\mathrm{f}} \approx 10^5 \rho.$$

Now most metal oxides have much larger resistivity than predicted by this equation. For example, aluminum oxide

has $\rho_f \approx 10^{12}$ Ωm (see Ref. [32]) compared to the resistivity of aluminum which is $\rho \approx 3 \times 10^{-8}$ Ωm. However, if the aluminum oxide film is thin enough electrons can tunnel through it which could give a smaller effective film resistance. However, estimation of this for typical thickness of aluminum oxide films ($d \approx 3$ nm) still gives a resistivity (of order $\rho_f \approx 10^6$ Ωm) much larger than $10^5\rho$ (see Ref. [33]). We conclude that unless the oxide film is very imperfect (with could allow sequential or resonant tunneling, or the formation of metallic channels [33]), the oxide film must be broken in order for the constriction resistance to dominate the contact resistance.

Up to now we have assumed that the power spectrum has a roll-off and that the nominal contact area is so large (linear size L) that π/L is a wavenumber in the roll-off region. In many electrical contacts problem the nominal contact region is very small in order to get high enough contact pressure to break (or penetrate) the oxide and contamination films. In these cases a single macroscopic sized contact region may form. In particular if one surface has a spherical curvature (radius of curvature R) the macroscopic contact pressure would be Hertz-like assuming no plastic deformation on the macroscopic scale.

If the Hertz theory can be applied the diameter D of the contact region depends on the normal force as $D \sim F^{1/3}$ and in this limit the contact resistance $R \sim F^{-1/3}$. If instead the contact area is fully plastically deformed the contact diameter is determined by $4F/(\pi D^2) = \sigma_P$, where σ_P is the penetration hardness, and the contact resistance $R \sim F^{-1/2}$.

To avoid or reduce the influence of oxide and contamination films the contacting surfaces are often covered by thin gold films. Gold is the only metal which does not react with atmospheric gases and no oxide (or sulfide) film form on the surface. In addition, gold is plastically soft (penetration hardness $\sigma_P \approx 0.2$ GPa) which result in a large contact area even at relative low contact pressures.

In some application only one of the contacting surfaces is covered by a gold film. This can result in problems as illustrated in Fig. 6 for the contact between a gold covered steel surface and an aluminum surface with an oxide film. Since the penetration hardness of gold is rather low the contact stress may not be high enough to break the oxide film resulting in a huge contact resistance (which may be determined by electron tunneling through the oxide film). To break the oxide film I suggest to include hard metallic particles in the gold film. This would result in very large local contact stresses which could break the oxide film and allow gold to be squeezed in contact with the aluminum. If the electric current is of the DC type and in the right direction electromigration could fill up the cracks with gold as indicated in Fig. 6

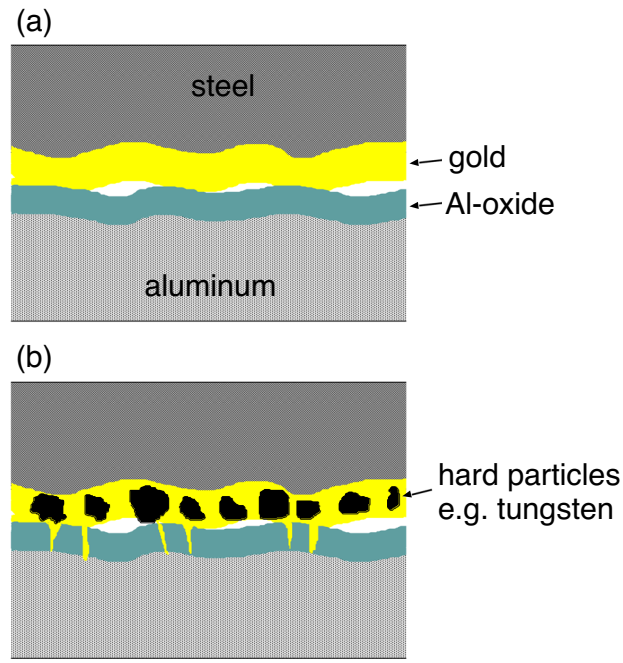

Fig. 6 A gold covered steel surface squeezed against an aluminum surface with an oxide film. **a** The penetration hardness of gold is rather low (about 200 MPa) and may not be enough to break the oxide film resulting in a huge contact resistance. **b** By including hard metallic particles in the gold film very large local contact stresses may occur which could break the oxide film and allow gold to be squeezed in contact with the aluminum

In this paper, we have assumed that the electron transfer in the junctions are diffusive i.e. the electron mean free path is smaller than the diameter (and length) of the constructions. For most practical systems this is likely to be the case owing to oxide fragments and contamination molecules embedded in the junction material at the contacting interface. This is likely to be the case even for gold contacts in the normal atmosphere. However, for very clean metallic surfaces, in particular gold in vacuum condition, very thin conducting junctions may form where the electron transfer is ballistic rather than diffusive. In this case the resistance of the individual junctions may be quantized in the units of $h/(2e^2) \approx 1.3 \times 10^4$ Ω (where h is Planck constant and e the electron charge) [34, 35]. However, even in these cases for surfaces with roughness on many length scales and high enough applied normal force (as is relevant for most electronic applications) the contact resistance will be determined by the macroscopic contact stiffness and the long wavelength surface roughness, and the exact origin of the microscopic electron transfer (which could be diffusive or ballistic) is irrelevant for contact resistance.

Finally I note that there are several important effects we have not discussed above. Thus, the contact resistance result

in energy dissipation and local temperature increase at the junctions [3, 36]. Because of the surface roughness the contact will have capacitance, and electrostatic attraction will occur between the bodies. This *electroadhesion* depends on the probability distribution of surface separation [37, 38]. Associated with the conducting constrictions will also be an inductance [3]

10 Summary and Conclusion

The nature of the electric contact between two contacting metallic bodies is a fundamental problem which has been studied for a long time. Almost all studies today are based on the classical constriction approach which is summarized in the book of Holm [3]. However, an alternative theory which is simpler and formally exact was developed by Barber [5]. In this theory the constriction resistance is shown to be proportional to the mechanical contact stiffness which usually is determined by the most long wavelength roughness. In this paper I have shown how these two very different approaches are related. I have presented an analytical formula for the contact stiffness covering all contact pressures above the pressure range where finite-size effects are important. I have also suggested a way to improve the contact resistance when one of the contacting solids is covered by a gold film, by incorporating hard metallic (e.g. tungsten) particles in the gold film, which can break the oxide film on the counter surface.

Acknowledgements I thank J.R. Barber and E. Tosatti for comments on the text.

Funding Open Access funding enabled and organized by Projekt DEAL. The authors have not disclosed any funding.

Declarations

Conflict of interest The author declare no conflict of interest in this study.

Open Access This article is licensed under a Creative Commons Attribution 4.0 International License, which permits use, sharing, adaptation, distribution and reproduction in any medium or format, as long as you give appropriate credit to the original author(s) and the source, provide a link to the Creative Commons licence, and indicate if changes were made. The images or other third party material in this article are included in the article's Creative Commons licence, unless indicated otherwise in a credit line to the material. If material is not included in the article's Creative Commons licence and your intended use is not permitted by statutory regulation or exceeds the permitted use, you will need to obtain permission directly from the copyright holder. To view a copy of this licence, visit http://creativecommons.org/licenses/by/4.0/.

References

1. See http://www.pepbrainin.com/technical-resources/troubleshooting-common-electrical-contact-problems/
2. Holm, R.: Wiss. Veröff Siemens-Werken **7**, 217 (1929)
3. Holm, R.: Electric Contacts Handbook. Springer, Berlin (1967)
4. Greenwood, J.A.: Constriction resistance and the real area of contact. J. Appl. Phys. **17**, 1621 (1966)
5. Barber, J.R.: Bounds on the electrical resistance between contacting elastic rough bodies. Proc. R. Soc. Lond. Ser. A **459**, 53 (2003)
6. Barber, J.R.: Contact Mechanics, 1st edn. Springer, Berlin (2018)
7. Persson, B.N.J.: Theory of rubber friction and contact mechanics. J. Chem. Phys. **115**, 3840 (2001)
8. Persson, B.N.J.: Relation between interfacial separation and load: a general theory of contact mechanics. Phys. Rev. Lett. **99**, 125502 (2007)
9. Persson, B.N.J.: Contact mechanics for randomly rough surfaces. Surf. Sci. Rep. **61**, 201 (2006)
10. Almqvist, A., Campana, C., Prodanov, N., Persson, B.N.J.: Interfacial separation between elastic solids with randomly rough surfaces: comparison between theory and numerical techniques. J. Mech. Phys. Solids **59**, 2355 (2011)
11. Afferrante, L., Bottiglione, F., Putignano, C., Persson, B.N.J., Carbone, G.: Elastic contact mechanics of randomly rough surfaces: an assessment of advanced asperity models and Persson's theory. Tribol. Lett. **66**, 1 (2018)
12. Persson, B.N.J., Albohr, O., Tartaglino, U., Volokitin, A.I., Tosatti, E.: On the nature of surface roughness with application to contact mechanics, sealing, rubber friction and adhesion. J. Phys. Condens. Matter **17**, R1 (2004)
13. Persson, B.N.J.: On the fractal dimension of rough surfaces. Tribol. Lett. **54**, 99 (2014)
14. Jacobs, T.D.B., Junge, T., Pastewka, L.: Quantitative characterization of surface topography using spectral analysis. Surf. Topogr. Metrol. Prop. **5**(1), 013001, 013001 (2017)
15. Hyun, S., Pei, L., Molinari, J.F., Robbins, M.O.: Phys. Rev. E **70**, 026117 (2004)
16. Müser, M.H., Wang, A.: Contact-patch-size distribution and limits of self-affinity in contacts between randomly rough surfaces. Lubricants **6**, 85 (2018)
17. Prodanov, N., Dapp, W.B., Müser, M.H.: On the contact area and mean gap of rough, elastic contacts: dimensional analysis, numerical corrections, and reference data. Tribol. Lett. **53**, 433 (2014)
18. Pastewka, L., Prodanov, N., Lorenz, B., Müser, M.H., Robbins, M.O., Persson, B.N.J.: Finite-size scaling in the interfacial stiffness of rough elastic contacts. Phys. Rev. E **87**, 062809 (2013)
19. Pohrt, R., Popov, V.L.: Normal contact stiffness of elastic solids with fractal rough surfaces. Phys. Rev. Lett. **108**, 104301 (2012)
20. Campana, C., Persson, B.N.J., Müser, M.H.: Transverse and normal interfacial stiffness of solids with randomly rough surfaces. J. Phys. Condens. Matter **23**, 085001 (2011)
21. Lorenz, B., Persson, B.N.J.: Interfacial separation between elastic solids with randomly rough surfaces: comparison of experiment with theory. J. Phys. Condens. Matter **21**, 015003 (2008)
22. Wang, D., Ueckermann, A., Schacht, A., Oeser, M., Steinauer, B., Persson, B.N.J.: Tire-road contact stiffness. Tribol. Lett. **56**, 397 (2014)
23. Parel, K.S., Paynter, R.J., Nowell, D.: Linear relationship of normal and tangential stiffness with load. Proc. R. Soc. Lond. **476**, 2243 (2020)
24. Berthoud, P., Baumberger, T.: Proc. R. Soc. A **454**, 1615 (1998)
25. Persson, B.N.J., Lorenz, B., Volokitin, A.I.: Heat transfer between elastic solids with randomly rough surfaces. Eur. Phys. J. E **31**, 3 (2010)

26. Volokitin, A.I., Persson, B.N.J.: Near-field radiative heat transfer and noncontact friction. Rev. Mod. Phys. **79**, 1291 (2007)
27. Volokitin, A.I., Persson, B.N.J.: Electromagnetic Fluctuations at the Nanoscale: Theory and Applications. Springer, Berlin, Heidelberg (2017)
28. Kottler, F.: Electrostatik der Leiter. Handbuch der Physik von Geiger und Scheel, Bd. 12. Springer, Berlin (1927)
29. Greenwood, J.A., Williamson, J.B.P.: Contact of nominally flat surfaces. Proc. R. Soc. Lond. Ser. A Math. Phys. Sci. **295**, 300 (1966)
30. Müser, M.H., et al.: Meeting the contact-mechanics challenge. Tribol. Lett. **65**, 118 (2017)
31. Persson, B.N.J.: Sliding Friction, Physical Principles and Applications, 2nd edn. Springer, Berlin (2000)
32. See https://hypertextbook.com/facts/2006/EuniceHuang.shtml
33. Cyster, M.J., Smith, J.S., Vaitkus, J.A., Vogt, N., Russo, S.P., Cole, J.H.: Effect of atomic structure on the electrical response of aluminum oxide tunnel junctions. Phys. Rev. Res. **2**, 013110 (2020)
34. Requist, R., Baruselli, P.P., Smogunov, A., Fabrizio, M., Modesti, S., Tosatti, E.: Metallic, magnetic and molecular nanocontacts. Nat. Nanotechnol. **11**, 499 (2016)
35. Khosravi, A., Laine, A., Vanossi, A., Wang, J., Siria, A., Tosatti, E.: Understanding the rheology of nanocontacts. Nat. Commun. **13**, 2428 (2022)
36. Kohlrausch, F.: Über den stationären Temperaturzustand eines elektrisch geheizten Leiters. Ann. Phys. Lpz. **1**, 132 (1900)
37. Persson, B.N.J.: The dependency of adhesion and friction on electrostatic attraction. J. Chem. Phys. **148**, 144701 (2018)
38. Sirin, O., Ayyildiz, M., Persson, B.N.J., Basdogan, C.: Electroadhesion with application to touchscreens. Soft Matter **15**, 1758 (2019)

Publisher's Note Springer Nature remains neutral with regard to jurisdictional claims in published maps and institutional affiliations.